PAPER

Check for updates

Constructing recyclable biomass-derived thermosetting polymers *via* a solvent-free and catalyst-free Knoevenagel condensation reaction

Yaowei Zhu, [ID] [a,c] Tongtong Man,[a] Jiayi Chen,[a] Xiaonong Zhang,[b] Mingming Zhao,[b] Li Chen [ID] *[a] and Chunsheng Xiao [ID] *[b]

The extensive utilization of thermosetting polymers has prompted growing environmental concerns due to their non-recyclability and resource depletion. To address these challenges, the development of eco-friendly synthetic strategies for creating recyclable thermosetting polymers is imperative. Herein, we developed a solvent-free and catalyst-free synthesis approach to prepare recyclable biomass-derived thermosetting polymers using the dynamic Knoevenagel condensation (KC) reaction. We demonstrated that the dynamic exchange of C=C bonds could occur *via* the KC reaction at 110 °C without the need for solvents or catalysts. The thermosetting polymer BFMD-PCLT was then synthesized *via* the solvent-free and catalyst-free KC reaction. The resulting BFMD-PCLT exhibited an elongation at break of 184%, a tensile strength of 3.6 MPa, and exceptional fatigue resistance (withstanding ≥500 stretching cycles). Furthermore, BFMD-PCLT demonstrated high thermal stability (up to 275 °C) alongside excellent reprocessability and chemical recyclability. Overall, this research provides an eco-friendly, facile, and sustainable approach for creating recyclable biomass-derived thermosetting polymers.

Green foundation

1. Our work provides an eco-friendly and sustainable approach for creating recyclable biomass-based thermosetting polymers *via* a solvent-free and catalyst-free Knoevenagel condensation (KC) reaction.

2. We demonstrate that the biomass-based thermosetting polymer BFMD-PCLT could be facilely synthesized without solvents/catalysts at 110 °C. The resulting BFMD-PCLT exhibits chemical recyclability, reprocessability, and exceptional fatigue resistance (withstanding ≥500 stretching cycles).

3. Further research should focus on developing greener monomers derived from biomass sources to prepare various sustainable polymer materials.

Introduction

The application of thermosetting polymers, which cannot be reworked or recycled, has raised significant concerns regarding environmental pollution and resource wastage.[1–5] To address these challenges, researchers integrated biomass materials into polymer synthesis as sustainable alternatives to non-renewable fossil resources, aiming to enhance the sustainability of polymer production.[6–8] Currently, various biomass materials, including vegetable oil, cellulose, sugars, and natural rubber, are utilized in the synthesis of thermosetting polymers.[9,10] These feedstocks are primarily derived from agricultural crops, forestry residues, and organic waste and are produced through processes like extraction, fermentation, and chemical treatment, making them integral to a circular bioeconomy.[11,12] However, similar to conventional thermosets, most biomass-derived thermosets face challenges in reprocessing and recycling due to their permanent cross-linked structure.[13]

Recently, the incorporation of dynamic covalent bonds (DCBs) into cross-linking networks has proven to be an effective method for fabricating thermosetting polymers that can be reprocessed and recycled.[14–26] Therefore, the use of biomass materials combined with DCBs for creating recyclable thermoset polymer materials has garnered considerable attention. In our previous work, the C=C bonds formed through the Knoevenagel condensation (KC) reaction have been employed for constructing dynamic hydrogels in aqueous media and thermosetting polymers in organic solvents under catalysis of 4-dimethylaminopyridine (DMAP).[27–31] These

[a] Department of Chemistry, Northeast Normal University, Changchun 130024, P. R. China. E-mail: chenl686@nenu.edu.cn
[b] State Key Laboratory of Polymer Science and Technology, Key Laboratory of Polymer Ecomaterials, Changchun Institute of Applied Chemistry, Chinese Academy of Sciences, Changchun 130022, P. R. China. E-mail: xiaocs@ciac.ac.cn
[c] College of Chemistry and Chemical Engineering, Taishan University, Tai'an 271000, PR China

studies demonstrate the significant potential of KC reactions in creating recyclable biomass thermosetting polymers. However, most KC products still require an additional catalyst to facilitate the dynamic exchange of C=C bonds.[32,33] The utilization of catalysts in the synthesis of thermosetting polymers can present challenges such as compatibility issues and potential toxicity concerns. In specific applications like coatings, excessive catalyst concentrations can potentially cause substrate corrosion.[34–39] Moreover, the properties of thermosetting polymers can also be influenced by residual solvents. Consequently, the development of solvent-free and catalyst-free thermosetting polymers has garnered significant attention in recent years. Our previous research has demonstrated that the Knoevenagel condensation reaction using cyanoacetate can proceed without a catalyst.[27] Furthermore, it has been reported that the solvent-free KC reaction can be successfully conducted.[40–43] Thus, it is feasible to synthesize recyclable thermosetting polymers derived from biomass materials *via* the KC reaction without a solvent and catalyst.

In this work, we developed a solvent-free and catalyst-free KC reaction-based strategy to create the biomass-derived thermosetting polymer BFMD-PCLT through the successful crosslinking of bis((5-formylfuran-2-yl)methyl)decanedioate (BFMD) and trifunctionalized monomers (PCL-TCA) (Scheme 1). Two biomass-derived monomers, 5-hydroxymethylfurfural (HMF) and sebacic acid, can be produced from glucose (*via* dehydration)[44] and castor oil (*via* pyrolysis),[45] respectively. Through this novel KC reaction, it is possible to produce a thermosetting polymer with a high molecular weight and successfully enable dynamic exchange of C=C bonds within the polymers. The obtained BFMD-PCLT exhibits excellent mechanical properties, fatigue resistance, reprocessing and chemical recycling capabilities. Additionally, it can be used to prepare weldable polymer wires. Overall, the present work demonstrates that the KC reaction can proceed without a solvent and catalyst, which thereby provides a powerful tool for preparing sustainable materials.

Results and discussion

Solvent-free and catalyst-free KC reaction and dynamic exchange

To verify the feasibility of constructing recyclable biomass-derived thermosetting polymers through the KC reaction without a solvent and catalyst, hexyl cyanoacetate (HCA) and (5-formylfuran-2-yl)methyl hexanoate (FMH) were first selected for a model reaction. And the theoretical product of this model reaction, *i.e.*, (E)-(5-(2-cyano-3-(hexyloxy)-3-oxoprop-1-en-1-yl)furan-2-yl)methyl hexanoate (CHFMH), was also synthesized. The structures of HCA, FFMH, and CHFMH were characterized by hydrogen nuclear magnetic resonance (^{1}H NMR) spectroscopy (Fig. S1–S3).

Then, we simply mixed FFMH and HCA through heating to facilitate the reaction. The process of the model reaction was monitored by ^{1}H NMR spectroscopy at room temperature, 70, 90, and 110 °C. At room temperature, there is no significant change observed in the ^{1}H NMR spectra of FFMH and HCA
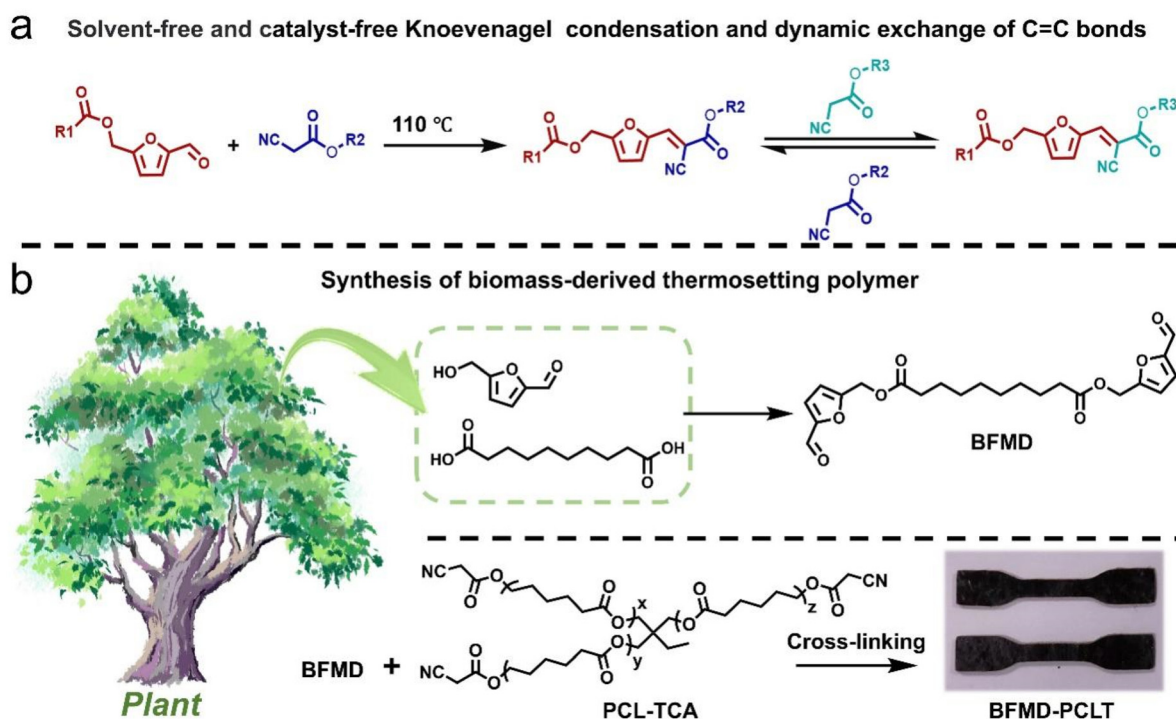
Scheme 1 (a) Solvent-free and catalyst-free KC reaction and the dynamic exchange of C=C bonds. (b) Synthesis route to a biomass-derived thermosetting polymer.

mixtures within 120 min (Fig. S4), indicating that the solvent-free and catalyst-free KC reaction cannot occur at room temperature.

In contrast, this solvent-free and catalyst-free KC reaction can be effectively conducted upon increasing the temperature. For example, the process of the model reaction at 110 °C was analyzed using ^{1}H NMR spectra. As shown in Fig. 1, the intensities of proton resonance peaks 3 (–CHO on FFMH, at 9.65 ppm) and 4 (CN–CH$_2$– on HCA, at 3.47 ppm) gradually decreased with the reaction time prolonging, while the proton resonance peak III (–C=CH– on CHFMH, at 8.01 ppm) increased over time, demonstrating the consumption of FFMH and HCA and the formation of CHFMH. Meanwhile, proton resonance peaks 1 (–CH=CH–, on FFMH, at 6.60 ppm) and 2 (–CH=CH–, on FFMH, at 7.22 ppm) moved to peaks I (–CH=CH– on CHFMH, at 6.65 ppm) and II (–CH=CH– on CHFMH, at 7.43 ppm), respectively. The proton resonance peak 5 (–CH$_2$–O–C=O on HCA, at 4.22 ppm) moved to peak IV (–CH$_2$–O–C=O on CHFMH, at 4.30 ppm). The observed chemical shift of the proton peaks I, II, and IV towards the lower field can be attributed to the electron-withdrawing effect induced by the newly formed C=C bond in CHFMH. As shown in Fig. S5 and S6, similar changes can also be observed at both 70 and 90 °C. And the KC reaction rate increases with rising temperature (Fig. S7). And the corresponding quantitative conversion data are listed in Table S1. These results demonstrate that solvent-free and catalyst-free KC reaction can be successfully performed through heating.

To verify the dynamic KC reaction under solvent-free and catalyst-free conditions, the dynamic exchange reaction of (E)-(5-(2-cyano-3-methoxy-3-oxoprop-1-en-1-yl)furan-2-yl)methyl hexanoate (CMFMH) and HCA was investigated by ^{1}H NMR spectroscopy. CMFMH was synthesized by a solvent-free and catalyst-free KC reaction, and its structure was characterized by ^{1}H NMR and ^{13}C NMR spectroscopy (Fig. S8 and S9). As shown in Fig. 2, there were obvious changes in the proton resonance

peak after only 10 min of reaction. The proton resonance peak was shifted from peak 1 (CN–C=CH– on CMFMH, at 8.02 ppm) to peak I (CN–C=CH– on CHFMH, at 8.01 ppm), and the proton resonance peak 3 (–CH$_2$–O– on HCA, at 4.22 ppm) was moved to peak III (–CH$_2$–O– on CHFMH, at 4.30 ppm). These results demonstrate that CMFMH was transformed into CHFMH. In addition, the intensity of peak 2 (–O–CH$_3$ on CHFMH, at 3.93 ppm) gradually decreased, which proved that the content of CMFMH in the reaction system decreased gradually. The appearance of the proton resonance peak II (–O–CH$_3$ on methyl cyanoacetate, at 3.85 ppm) confirmed the presence of free methyl cyanoacetate (MCA) in the reaction system, thereby indicating the successful dynamic exchange between hexyl cyanoacetate and CHFMH through the exchange of C=C bonds. The disappearance of peak II at 120 min was attributed to the evaporation of MCA with a low boiling point. Upon heating the model reaction mixture for 480 min, negligible changes were observed in the ^{1}H NMR spectra, thereby confirming the good thermal stability of CMFMH and CHFMH, and the formation of MCA can be attributed to the dynamic exchange of C=C bonds rather than potential thermal decomposition of CMFMH. These results demonstrate the efficient dynamic exchange of C=C bonds based on the KC reaction, even under solvent-free and catalyst-free conditions.

Preparation and dynamic exchange of linear polymers

To verify catalyst-free and solvent-free Knoevenagel polycondensation and dynamic exchange in polymers, we further synthesized bis((5-formylfuran-2-yl)methyl)decanedioate (BFMD), polycaprolactone bis(2-cyanoacetate) (PCL-BCA), and a linear
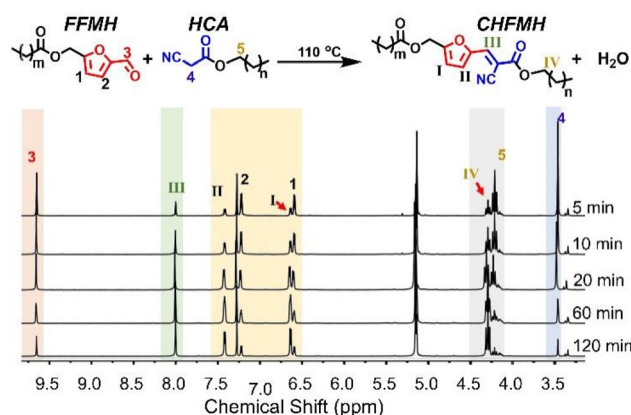

Fig. 1 Time-dependent ^{1}H NMR spectra of a solvent-free and catalyst-free KC reaction at 110 °C (the molar ratio of FFMH to HCA is 1:1, m = 5, n = 4). The reaction was monitored by ^{1}H NMR spectroscopy at 5, 10, 20, 60, and 120 min in CDCl$_3$.
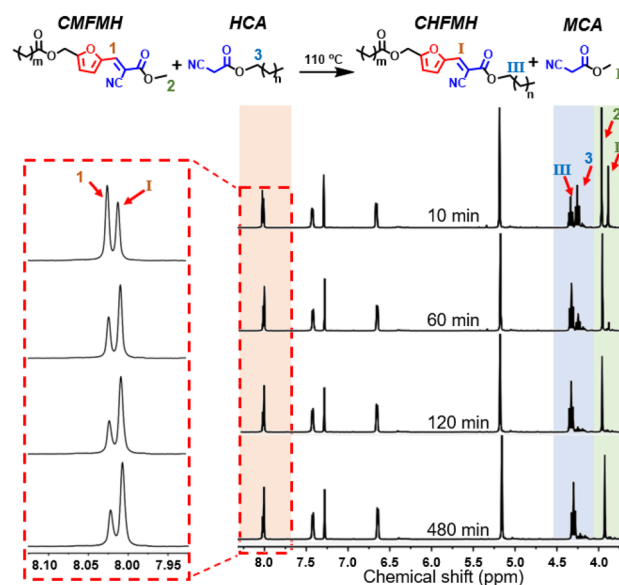

Fig. 2 The dynamic exchange of C=C bonds of CMFMH and HCA at 110 °C (the molar ratio of CMFMH to HCA is 1:0.7, m = 5, n = 4). The reaction was monitored by ^{1}H NMR spectroscopy at 10, 60, 120, and 480 min.

polymer model (BFMD-PCLT). Their structures were characterized by ^{1}H NMR spectroscopy (Fig. S10–12). Based on BFMD and di-functionalized polycaprolactone (PCL-BCA), the Knoevenagel polycondensation and dynamic exchange reactions were performed, and the reaction routes are shown in Fig. 3a(I). BFMD and PCL-BCA were simply mixed at a molar ratio of 1 : 1 and then reacted without a solvent and catalyst.

The molecular weight (M_n) of BFMD-PCL was monitored by gel permeation chromatography (GPC). The Knoevenagel polycondensation proceeded quickly, with M_n reaching 43 kDa after 90 min (Fig. 3b). This result demonstrates the feasibility of achieving a high molecular-weight polymer through solvent-free and catalyst-free Knoevenagel polycondensation. Subsequently, PCL-BCA (0.5 equiv.) was added to the reaction system (Fig. 3a(II)), and the M_n of BFMD-PCLT first decreased sharply to 7 kDa and then increased slightly to 12 kDa (Fig. 3c). The significant decrease in M_n can be attributed to the formation of oligomers resulting from C=C bond exchange between PCL-BCA and BFMD-PCLT. After that, PCL-BCA continued to react with potential functional groups within the oligomers, leading to a slight increase in M_n and reaching an "equilibrium" state after 40 min. Next, when BFMD (0.5 equiv.) was added to the reaction system (Fig. 3a (III)), M_n could recover to 42 kDa after 90 min (Fig. 3d), which was close to the M_n of initial BFMD-PCL (Fig. 3b). This phenomenon is attributed to the continuous polycondensation of the 2-cyanoacetate end-functionalized oligomers with BFMD, and in this case, the molar ratio of BFMD and PCL-BCA (1 : 1) was the same as that in the initial state. Finally, when HCA (0.5 equiv.) was added to the reaction system, M_n remarkably decreased to 4.6 kDa after 20 min (Fig. 3a(IV) and

e). All the molecular weight data from GPC-THF analysis are listed in Table S2. Taken together, these results demonstrate that it is feasible to create dynamic polymers through solvent-free and catalyst-free Knoevenagel polycondensation.

Preparation, characterization, and recycling of crosslinked thermosetting polymers

The aforementioned experiments have demonstrated the successful preparation of the dynamic polymer through a solvent-free and catalyst-free KC reaction. Consequently, it is realistic to create dynamic thermosetting polymers through this solvent-free and catalyst-free KC reaction. We used cyanoacetic acid modified polycaprolactone triol (PCL-TCA) and BFMD to construct the thermosetting polymer BFMD-PCLT (Fig. 4a). The structures of PCL-TCA were characterized using ^{1}H NMR, ^{13}C NMR and Fourier transform infrared (FT-IR) spectra (Fig. S13, S14 and Fig. 4b). In the FT-IR spectrum of BFMD, two characteristic carbonyl stretching vibrations (C=O) can be clearly observed. The strong absorption at ~1730 cm^{-1} is assigned to the ester carbonyl group. The strong absorption at ~1670 cm^{-1} is assigned to the aldehyde carbonyl group. The significant redshift of the aldehyde peak from the typical range (~1730 cm^{-1}) is a direct consequence of the strong conjugation between the formyl group and the electron-rich furan ring. After the polymerization reaction, the spectrum of BFMD-PCLT shows significant changes: the characteristic peak of the aldehyde carbonyl at ~1670 cm^{-1} has virtually disappeared and a new peak emerges at ~1610 cm^{-1}. This is assigned to the newly formed C=C bond generated by the condensation. The ester carbonyl peak remains and appears as a broadened signal, confirming the integrity of the ester lin-
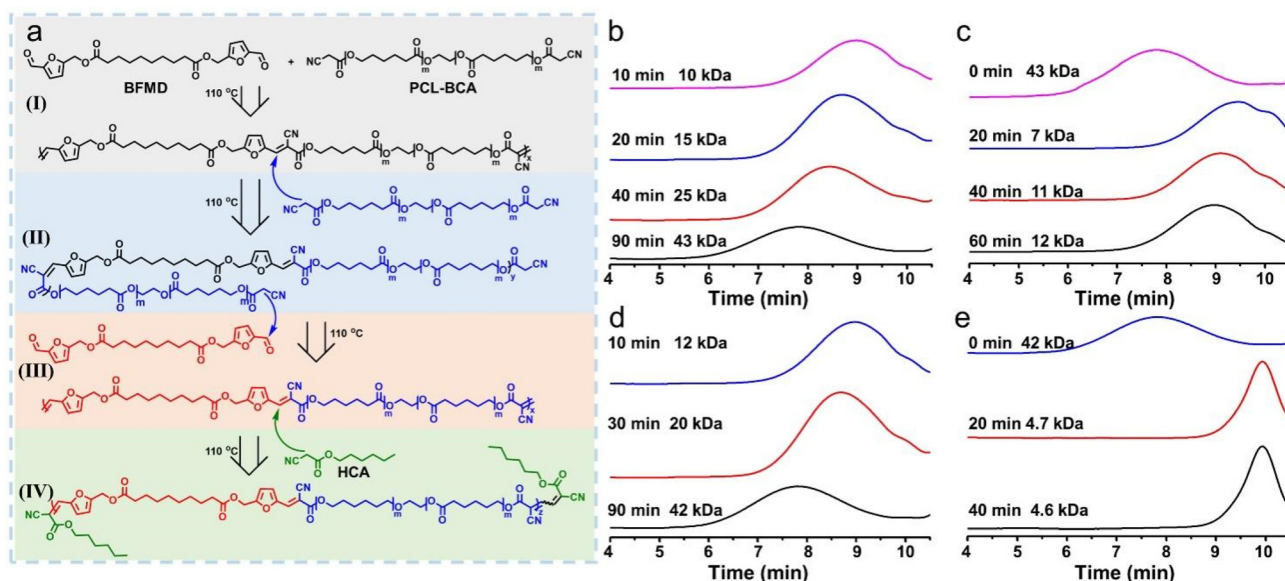

Fig. 3 GPC test of a linear polymer model (BFMD-PCLT) before and after dynamic exchange under solvent-free and catalyst free conditions. (a) Reaction routes of polycondensation and dynamic exchange. (I) Knoevenagel polycondensation of BFMD and PCL-BCA. (II) Addition of PCL-BCA to the reaction system. (III) Addition of BFMD to the reaction system. (IV) Addition of HCA to the reaction system. (b–e) GPC tests to monitor the changes in MP during reactions I–IV.
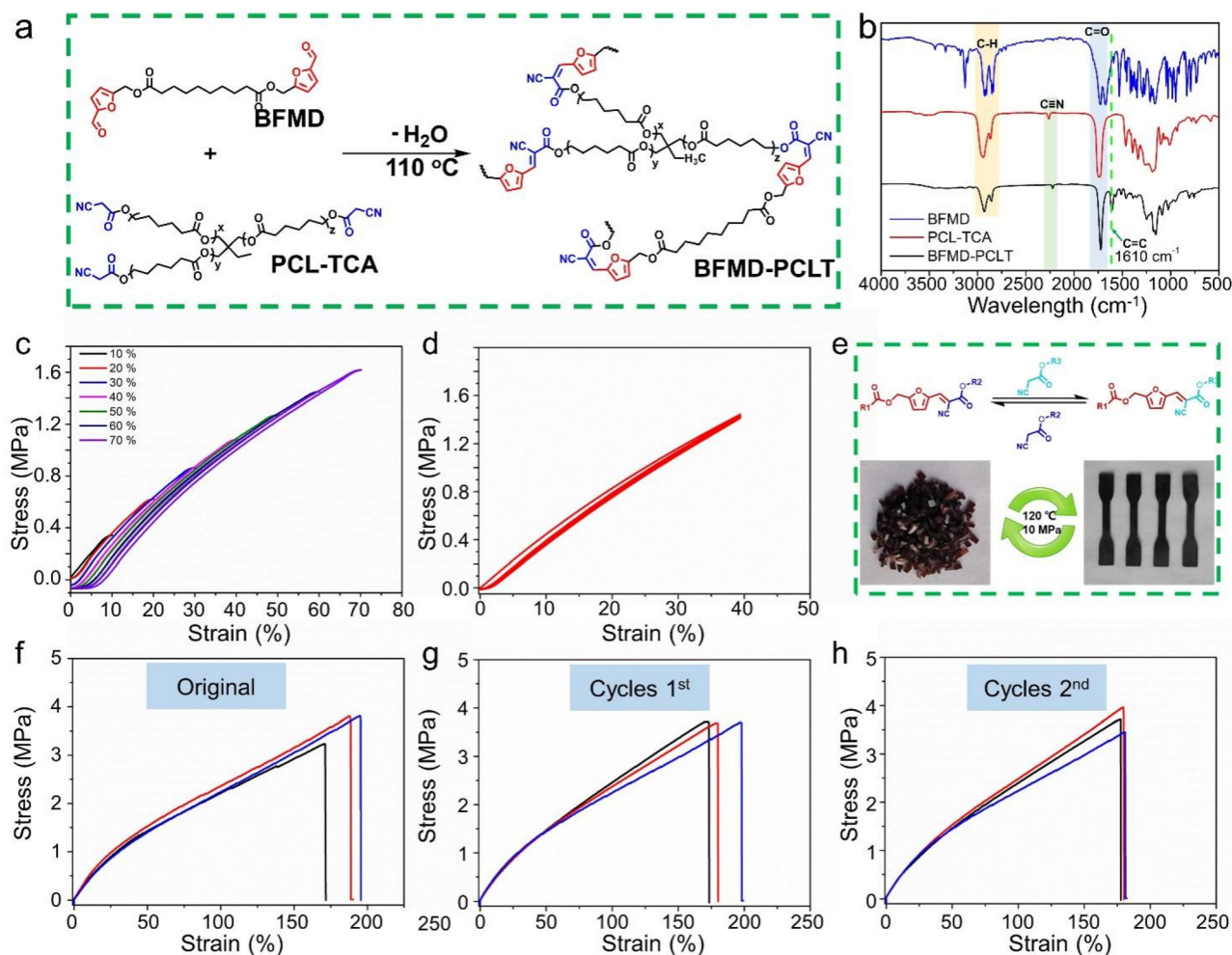
Fig. 4 (a) The synthetic route to BFMD-PCLT. (b) The FT-IR spectra of PCL-TCA, BFMD, and BFMD-PCLT. (c) Continuous tensile curves of BFMD-PCLT at different strains (10%–70%). (d) 500 loading–unloading tensile curves of BFMD-PCLT at a strain of 40% without any resting time. (e) Reprocessing of BFMD-PCLT based on the dynamic exchange of C=C bonds. Stress–strain curves of BFMD-PCLT with the number of hot-pressing cycles of original (f), 1 (g) and 2 (h).

kages in the resulting polymer. These spectral changes conclusively demonstrate the successful progression of the Knoevenagel condensation reaction.[27–30] The thermal properties of BFMD-PCLT were characterized by differential scanning calorimetry (DSC) and thermogravimetric analysis (TGA). The T_g of BFMD-PCLT under a nitrogen atmosphere was 0 °C (Fig. S15). The T_d (5%) of 275.5 °C indicates good initial thermal stability for the materials. The higher T_d (10%) of 345.5 °C suggests that after the initial weight loss the main polymer backbone remains stable until a substantially higher temperature before undergoing major decomposition. The residual mass of approximately 6% at 600 °C demonstrates a certain char-forming ability of the material (Fig. S16).

The degree of crosslinking was further determined by a swelling test of BFMD-PCLT. Common solvents, *i.e.*, dimethyl sulfoxide (DMSO), dichloromethane (DCM), *n*-hexane (C_6H_{14}), tetrahydrofuran (THF), water, and toluene (Tol), were used for these experiments (Fig. S17 and Table S3). The fragments of

BFMD-PCLT exhibited varying degrees of swelling across different solvents without dissolution (Fig. S17 and S18), proving the successful construction of a cross-linking network in BFMD-PCLT.[46] BFMD-PCLT exhibited significant swelling ratios in DMSO, DCM, and THF, which can be attributed to the good solubility of the PCL chains in these solvents.[46,47] Moreover, the gel fractions of BFMD-PCLT in different solvents are above 87% (Fig. S19). Overall, these findings indicate a substantial extent of cross-linking within BFMD-PCLT. The ^{1}H NMR analysis of the soluble fractions attributes the solvent discoloration to trace impurities, such as unreacted monomers and oligomers, rather than polymer degradation. This conclusion is supported by the detection of the corresponding residual functional groups in organic solvents and, critically, by the absence of any detectable signals in D_2O, which confirms the material's excellent hydrolytic stability (Fig. S20).

The mechanical properties of BFMD-PCLT were tested by a uniaxial tensile test. The as-synthesized BFMD-PCLT material

initially had an irregular morphology, which made it unsuitable for direct mechanical testing. To obtain standardized specimens for reliable and comparable tensile tests, the material was subjected to a hot-pressing process (110 °C, 10 MPa, 20 min). This hot-pressed sample was defined as the original sample for all subsequent testing and recycling cycles. At different strains ranging from 10% to 70%, BFMD-PCLT exhibited an insignificant hysteresis loop in each cycle (Fig. 4c), indicating the good resilience of BFMD-PCLT. To characterize the cycling stability of BFMD-PCLT, 500 uninterrupted cyclic tensile tests with strains of 40% without any rest time between cycles were further performed. These results show that the hysteretic loop of each cycle of BFMD-PCLT basically coincides with the first cycle (Fig. 4d), which proves that BFMD-PCLT exhibits a good anti-fatigue ability.

Subsequently, the original BFMD-PCLT was shredded and then reprocessed by compression molding (110 °C, 10 MPa, 20 min) (Fig. 4e). This process was repeated two times. A comparison of the FTIR spectra from the original BFMD-PCLT and those subjected to a hot-pressing cycle demonstrates the consistency of the chemical structure (Fig. S21). The mechanical properties of the materials were evaluated under identical conditions before and after reprocessing. The results show that the mechanical properties after two hot-pressing cycles are similar to those of the original material (Fig. 4f–h, and S22),

indicating that BFMD-PCLT has a good reprocessing ability. The relevant data are summarized in Table S4.

BFMD-PCLT can be chemically recycled though dynamic C=C bond exchange (Fig. 5a). The thermosetting polymers were first soaked in PCLTCA, and then, the mixture was heated to 110 °C and formed dark red viscous oil. These phenomena can be attributed to the transformation of the polymer network into low-molecular-weight oligomers via the dynamic exchange of C=C bonds between PCLTCA and BFMD-PCL.[30] Subsequently, BFMD was incorporated into the mixture at a molar ratio of 1 : 1 with PCLTCA. After heating for 4 h, the solidified mixture was compressed and restructured at 110 °C (Fig. 5b). The recycled polymer exhibited an identical FT-IR spectrum to the original BFMD-PCLT (Fig. 5c), which proved that its chemical structure did not change significantly. The tensile curves of the restructured BFMD-PCLT are shown in Fig. 5d. The reformed BFMD-PCLT show similar properties to the original BFMD-PCLT. Taken together, these results demonstrate that BFMD-PCLT exhibits excellent chemical recyclability. The relevant data are summarized in Table S5.

Application of BFMD-PCLT

Due to its excellent reprocessing ability, BFMD-PCLT is utilized as a flexible material for wire sheath preparation (Fig. 6a and b). BFMD-PCLT was processed into hollow polymer wire and
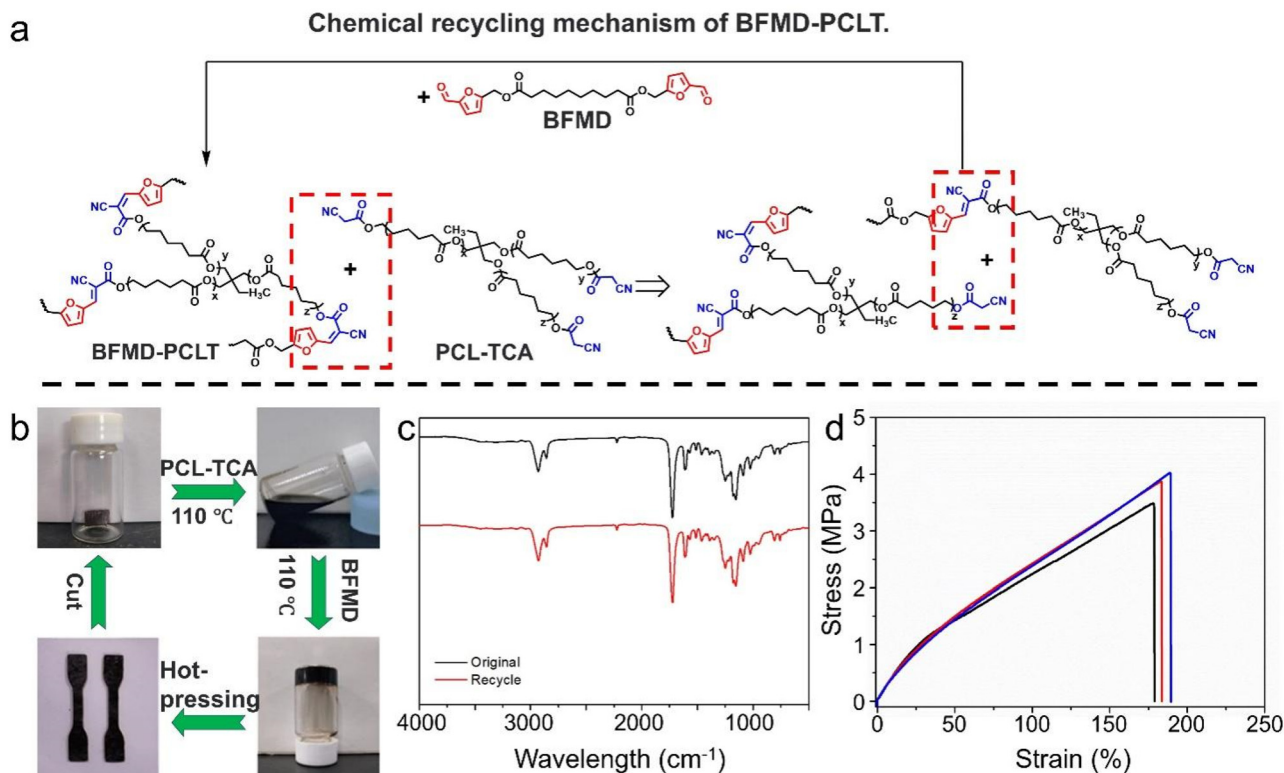

Fig. 5 (a) Chemical recycling mechanism of BFMD-PCLT. (b) Recycling and remolding processes of BFMD-PCLT. (c) FT-IR spectra of BFMD-PCLT before and after recycling. (d) Representative stress−strain curves of the restructured BFMD-PCLT.
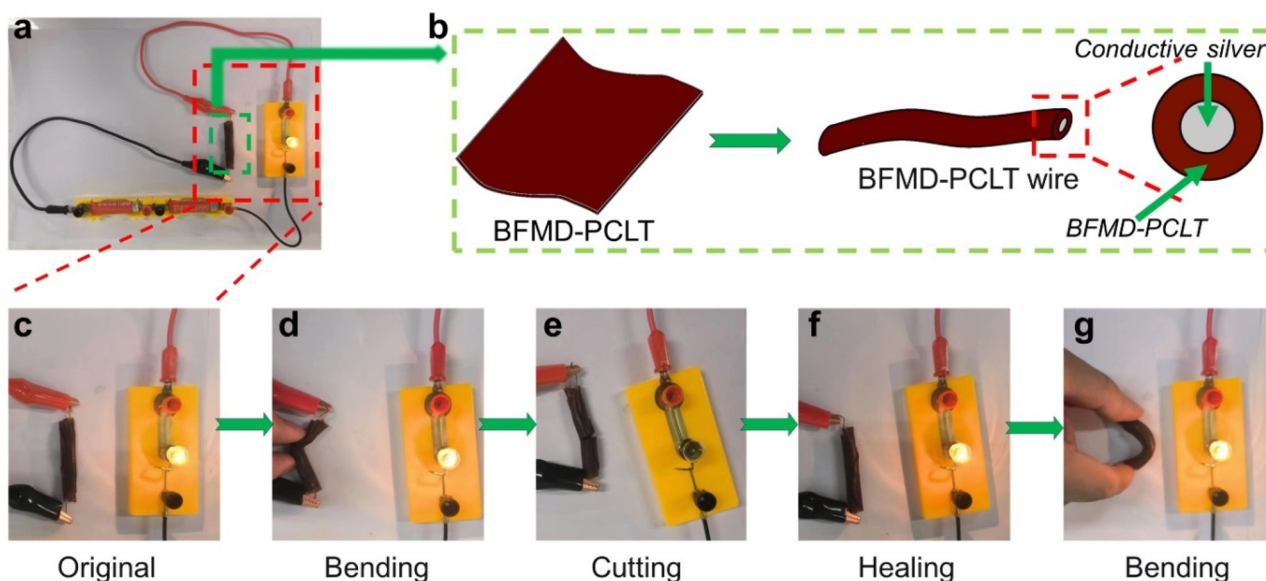
Fig. 6 Application of BFMD–PCLT as conductive wire. (a) Photo of a circuit containing a BMD–PCLT wire. (b) The process for preparing the BFMD–PCLT conductive wire. (c) Illumination occurs upon connection of the original conductive wire to a circuit. (d) The conductivity of the wire remains unaltered even after bending. (e) The light bulb goes out after the wire is cut. (f) Upon heating, the conductive wire undergoes self-healing, leading to circuit restoration. (g) The healed conductive wire retains conductivity even after bending.

filled with conductive silver, and the wire with BFMD-PCLT as the skin was fabricated. The wire was connected to a circuit and activated, resulting in the illumination of the bulb, indicating excellent conductivity of the wire (Fig. 6c). Even when bent, the wire maintained its conductivity (Fig. 6d). Subsequently, upon cutting off the wire, the circuit was disrupted and the bulb extinguished (Fig. 6e). Following alignment and heating at 110 °C for 2 hours, the incised wire underwent healing and regained its conductivity (Fig. 6f). The healed wire exhibited conductivity even after being subjected to bending (Fig. 6g). These experiments demonstrate significant potential of BFMD-PCLT in self-healable electronic devices.

Conclusions

In summary, we have developed an environmentally friendly method for synthesizing thermosetting polymers through solvent-free and catalyst-free KC reactions. The solvent-free and catalyst-free KC reaction of cyanoacetate with an aldehyde group was investigated at different temperatures. This KC reaction exhibited a temperature-dependent behaviour, the reaction rate increasing with temperature. The dynamic exchange of the C═C bond successfully proceeded without a solvent and catalyst at 110 °C. Through this solvent-free and catalyst-free KC reaction, the thermosetting polymer BFMD-PCLT was obtained by the KC reaction of BFMD and PCLTCA. The obtained BFMD-PCLT showed good mechanical properties and fatigue resistance and could be reprocessed and chemically recycled though dynamic C═C bond exchange. The intrinsic

reprocessability makes BFMD-PCLT suitable for use as the outer casing of weldable polymer wires. This work highlights the potential of the solvent-free and catalyst-free KC reaction for developing sustainable biomass-derived materials.

Experimental

The details of experiments are provided in the SI.

Author contributions

The manuscript was written through contributions of all authors. All authors have given approval to the final version of the manuscript.

Conflicts of interest

There are no conflicts to declare.

Data availability

All relevant data are available from the corresponding author upon reasonable request.

Supplementary information (SI) is available. See DOI: https://doi.org/10.1039/d5gc04302f.

Acknowledgements

References

1 Y. Jiang, J. Li, D. Li, Y. Ma, S. Zhou, Y. Wang and D. Zhang, *Chem. Soc. Rev.*, 2024, **53**, 624–655.

2 R. Auvergne, S. Caillol, G. David, B. Boutevin and J. P. Pascault, *Chem. Rev.*, 2014, **114**(2), 1082–1115.

3 A. Demongeot, R. Groote, H. Goossens, T. Hoeks, F. Tournilhac and L. Leibler, *Macromolecules*, 2017, **50**(16), 6117–6127.

4 R. L. Snyder, D. J. Fortman, G. X. De Hoe, M. A. Hillmyer and W. R. Dichtel, *Macromolecules*, 2018, **51**(2), 389–397.

5 R. Geyer, J. R. Jambeck and K. L. Law, *Sci. Adv.*, 2017, **3**(7), 1700782.

6 B. Zhang, Y. Jiang and R. Balasubramanian, *J. Mater. Chem. A*, 2021, **9**(44), 24759–24802.

7 Y. Zhu, C. Romain and C. K. Williams, *Nature*, 2016, **540**(7633), 354–362.

8 H. Feng, S. Ma, X. Xu, Q. Li, B. Wang, N. Lu, P. Li, S. Wang, Z. Yu and J. Zhu, *Green Chem.*, 2021, **23**(22), 9061–9070.

9 S. Kumar, S. K. Samal, S. Mohanty and S. K. Nayak, *Polym.-Plast. Technol. Eng.*, 2018, **57**(3), 133–155.

10 C. Veith, F. Diot-Néant, S. A. Miller and F. Allais, *Polym. Chem.*, 2020, **11**(47), 7452–7470.

11 M. Melikoglu, *Clean. Waste Syst.*, 2025, **12**, 100429.

12 A. Ali and J. D. Russell, *Curr. For. Rep.*, 2025, **11**(1), 1–20.

13 X. Zhao, P. Tian, Y. Li and J. Zeng, *Green Chem.*, 2022, **24**(11), 4363–4387.

14 Z. Lei, H. Chen, C. Luo, Y. Rong, Y. Hu, Y. Jin, R. Long, K. Yu and W. Zhang, *Nat. Chem.*, 2022, **14**(12), 1399–1404.

15 P. Chakma and D. Konkolewicz, *Angew. Chem., Int. Ed.*, 2019, **58**(29), 9682–9695.

16 D. Montarnal, M. Capelot, F. Tournilhac and L. Leibler, *Science*, 2011, **334**(6058), 965–968.

17 Y. Tian, L. Pang, R. Zhang, T. Xu, S. Wang, B. Yu, L. Gao, H. Cong and Y. Shen, *ACS Appl. Mater. Interfaces*, 2020, **12**(45), 50236–50247.

18 T. Guan, X. Wang, X. Zhao, X. Lu, X. Wang, Y. Wang and J. Sun, *CCS Chem.*, 2023, **6**(4), 1–28.

19 V. R. Sastri and G. C. Tesoro, *J. Appl. Polym. Sci.*, 1990, **39**(7), 1439–1457.

20 L. Imbernon, E. K. Oikonomou, S. Norvez and L. Leibler, *Polym. Chem.*, 2015, **6**(23), 4271–4278.

21 H. Guo, S. Huang, A. Xu and W. Xue, *Chem. Mater.*, 2022, **34**(6), 2655–2671.

22 P. Nellepalli, T. Patel and J. K. Oh, *Macromol. Rapid Commun.*, 2021, **42**(20), 2100391.

23 D. J. Fortman, J. P. Brutman, C. J. Cramer, M. A. Hillmyer and W. R. Dichtel, *J. Am. Chem. Soc.*, 2015, **137**(44), 14019–14022.

24 W. X. Liu, C. Zhang, H. Zhang, N. Zhao, Z. X. Yu and J. Xu, *J. Am. Chem. Soc.*, 2017, **139**(25), 8678–8684.

25 Y. Sun, Y. Y. Ren, Q. Li, R. W. Shi, Y. Hu, J. N. Guo, Z. Sun and F. Yan, *Chin. J. Polym. Sci.*, 2019, **37**, 1053–1059.

26 X. Lu, P. Xie, X. Xiang and J. Sun, *Macromolecules*, 2022, **55**(7), 2557–2565.

27 X. Ding, G. Li, P. Zhang and C. Xiao, *ACS Macro Lett.*, 2020, **9**(6), 830–835.

28 X. Ding, G. Li, P. Zhang, E. Jin, C. Xiao and X. Chen, *Adv. Funct. Mater.*, 2021, **31**(19), 2011230.

29 X. Ding, Y. Wang, J. Liu, P. Zhang, G. Li, T. Sun and C. Xiao, *Chem. Mater.*, 2021, **33**(15), 5885–5895.

30 Y. Zhu, T. Man, Y. Tian, X. Zhang, J. Liu, L. Chen and C. Xiao, *Macromolecules*, 2024, **57**(5), 1962–1969.

31 Y. Zhu, T. Man, M. Zhao, J. Chen, Y. Yan, X. Zhang, L. Chen and C. Xiao, *Chin. J. Polym. Sci.*, 2025, **43**, 53–60.

32 S. Xu, Z. Liao, A. Dianat, S. W. Park, M. A. Addicoat, Y. Fu, D. L. Pastoetter, F. G. Fabozzi and Y. Liu, *Angew. Chem., Int. Ed.*, 2022, **134**(21), e202202492.

33 S. Wang, H. Feng, J. Lim, K. Li, B. Li, J. J. Mah, Z. Xing, J. Zhu, X. J. Loh and Z. Li, *J. Am. Chem. Soc.*, 2024, **146**(14), 9920–9927.

34 N. Zheng, J. Hou, Y. Xu, Z. Fang, W. Zou, Q. Zhao and T. Xie, *ACS Macro Lett.*, 2017, **6**, 326–330.

35 B. Hendriks, J. Waelkens, J. M. Winne and F. E. Du Prez, *ACS Macro Lett.*, 2017, **6**(9), 930–934.

36 D. J. Fortman, J. P. Brutman, C. J. Cramer, M. A. Hillmyer and W. R. Dichtel, *J. Am. Chem. Soc.*, 2015, **137**(44), 14019–14022.

37 P. Taynton, K. Yu, R. K. Shoemaker, Y. Jin and W. Zhang, *Adv. Mater.*, 2014, **26**(23), 3938–3942.

38 M. Guerre, C. Taplan, R. Nicolaÿ, J. M. Winne and F. E. Du Prez, *J. Am. Chem. Soc.*, 2018, **140**(41), 13272–13284.

39 M. Röttger, T. Domenech, R. van Der Weegen, A. Breuillac, R. Nicolaÿ and L. Leibler, *Science*, 2017, **356**(6333), 62–65.

40 W. Wang, M. Luo, W. Yao, S. A. Pullarkat, L. Xu and P. H. Leung, *ACS Sustainable Chem. Eng.*, 2018, **7**(1), 1718–1722.

41 S. Kumar, *Green Process. Synth.*, 2014, **3**(3), 223–227.

42 B. Sen, S. Paul, P. Krukowski, D. Kundu, S. Das, P. Banerjee, M. Małecka, S. J. Abbas and S. I. Ali, *Inorg. Chem.*, 2024, **36**(6), 2919–2933.

43 L. Imbernon, S. Norvez and L. Leibler, *Macromolecules*, 2016, **49**(6), 2172–2178.

44 Z. Tang, J. Liang and J. Su, *Appl. Catal., A*, 2025, **696**, 120184.

45 S. Singh, S. Sharma, S. J. Sarma and S. K. Brar, *Environ. Prog. Sustainable Energy*, 2023, **42**(2), e14008.

46 Z. M. Png, J. Zheng, S. Kamarulzaman, S. Wang, Z. Li and S. S. Goh, *Green Chem.*, 2022, **24**(15), 5978–5986.

47 X. Liu, E. Zhang, J. Liu, J. Qin, M. Wu, C. Yang and L. Liang, *Chem. Eng. J.*, 2023, **454**, 139992.